Water Research 245 (2023) 120577

Contents lists available at ScienceDirect

Water Research

journal homepage: www.elsevier.com/locate/watres

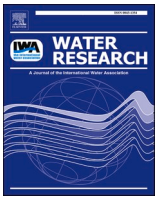

Development of The Navigator: A Lagrangian sensing system to characterize surface freshwater ecosystems

Aashish Khandelwal [a,*], Tzion Castillo [a,b], Ricardo González-Pinzón [a,*]

[a] Gerald May Department of Civil, Construction & Environmental Engineering, University of New Mexico, Albuquerque, NM, USA
[b] Electrical Engineering, University of New Mexico, Albuquerque, NM, USA

ARTICLE INFO

Keywords:
Lagrangian
Monitoring
Surface
Freshwater
Ecosystems
Water quantity and quality
Autonomous

ABSTRACT

Most freshwater aquatic studies rely on Eulerian monitoring, i.e., water quality and quantity are monitored using grab samples or semi-continuous sensors deployed at fixed cross-sections. While Eulerian monitoring is practical, it provides a limited understanding of spatial and temporal heterogeneity. We designed and built The Navigator, a Lagrangian (i.e., along a flow path) monitoring system that offers cost-effective solutions for in-situ, real-time data collection in surface freshwater ecosystems. The Navigator features a suite of technologies, including an autonomous surface vehicle with GPS and LTE connectivity, water quality sensors, a depth sonar, a camera, and a webpage dashboard to visualize real-time data. With these technologies, The Navigator provides insight into where, how, and why water quality and quantity change over time and space as it moves with the current or follows user-specified pathways. We tested The Navigator monitoring water quality parameters at high spatial-temporal resolution in multiple surface water bodies in New Mexico (USA) to: (1) identify water quality changes associated with land use changes along a 7th-order reach in the Rio Grande, (2) identify the fate of wildfire disturbances ~175 km downstream of a burned watershed affected by the largest wildfire ever recorded in the state, (3) monitor the water quality of a recreational fishing pond in the City of Albuquerque. Our three successful tests confirm that The Navigator is an affordable (USD 5,101 in 2023) monitoring system that can be used to address questions involving mass and energy balances in surface waters.

1. Introduction

Recent advances in high-resolution sensors, real-time telemetry, analytical equipment, and computer technology, among others, have sparked the 'renaissance of hydrology' (Gabrielle, 2019). In the context of surface water quality dynamics, this technological revolution has enabled the monitoring of multiple solutes across the periodic table (Abbott et al., 2018; Burns et al., 2019; Kirchner and Neal, 2013; Rode et al., 2016), in some cases at sub-hour resolutions (Jarvie et al., 2018; Lloyd et al., 2016; Nichols et al., 2022), and over multiple decades (Dupas et al., 2018; Huang et al., 2022; Li et al., 2020; Matson et al., 2021). However, due to affordability issues, those advances have contributed to an improved understanding and management of surface water resources only in a small number of watersheds across the globe (Arsenault et al., 2023; Devaraj et al., 2022). To date, thus, we still lack reliable, continuous, and consistent information on the extent and dynamics of surface water quantity and quality at local, regional, and global scales (United Nations Environment Programme, 2021). To tackle this shortcoming, the UN's sustainable development goal 6 (SDG6) aims to increase data availability for evidence-based management, regulations, and policymaking to "*ensure access to water and sanitation for all*".

While satellite observations can help monitor regional-to-continental scale processes (e.g., evapotranspiration, intercontinental water and dust fluxes) and help identify relevant large-scale features through synoptic analyses (e.g., anoxic zones, flooding, and hurricanes) (Arabi et al., 2020; Li et al., 2022; Román et al., 2019; Wieland and Martinis, 2019), the temporal and spatial resolution of their information is typically inadequate to support local-to-regional scale decision-making associated with the management of surface water resources (Manfreda et al., 2018; Tapley et al., 2019). These limitations have kept Eulerian monitoring, i.e., the tracking of water quantity and quality at a site and over time, as the current standard technique applied in consulting, research, and enforcement of regulations associated with freshwater resources (Doyle and Ensign, 2009).

Eulerian monitoring of surface freshwaters can be done through grab sampling followed by laboratory analyses or semi-continuous sensors in

* Corresponding authors.
E-mail addresses: ashkhandelwal@unm.edu (A. Khandelwal), gonzaric@unm.edu (R. González-Pinzón).

https://doi.org/10.1016/j.watres.2023.120577
Received 15 February 2023; Received in revised form 10 May 2023; Accepted 4 September 2023
Available online 4 September 2023

situ (e.g., optical and wet-chemistry sensors) and has been used to quantify water quantity and quality dynamics at sub-hour to monthly frequencies. Eulerian monitoring is spatially limited due to the sparseness of instrumented sites, and this is particularly inconvenient for analyses featuring highly heterogeneous and rapidly changing environments (Krause et al., 2015). Since Eulerian monitoring fundamentally integrates the spatial heterogeneity, dynamics, and watershed modifications upstream of the monitoring site (Ensign et al., 2017; González-Pinzón et al., 2019; Hensley et al., 2014; Kunz et al., 2017), this technique falls short when linking causation and correlation. Some of the most common examples of these challenges are differentiating between point and distributed sources of contamination in water quality assessments and separating rainfall, snowmelt, and groundwater contributions from stream flow measurements. Fundamentally, Eulerian monitoring faces two main limitations, i.e., the spatial scale of analysis is proportional to the distance between observation points and, in consequence, human-defined boundaries are introduced and segments, flow paths, or reaches with ecologically contrasting functioning become undistinguishable and are effectively aggregated (Ensign et al., 2017).

An alternative to overcoming some of the challenges of Eulerian (i.e., fixed-site variation in time analyses) and synoptic monitoring (i.e., near-instantaneous variations in space analyses) is the use of Lagrangian monitoring, where water parcels are tracked as they move through aquatic systems (i.e., variation in space-time). Lagrangian monitoring of surface waters can be done with crews sampling or monitoring from a moving vehicle (e.g., boat or kayak) or using instrumented autonomous surface vehicles (ASVs; also known as uncrewed surface vehicles USVs). Even though Lagrangian monitoring removes the need to pre-define spatial boundaries, due to logistic limitations, it only informs about environmental processes associated with the monitored flow paths and may not sample relevant spatial heterogeneity in adjacent, bypassed flow paths. Due to the intractability and remoteness associated with Lagrangian monitoring, and high personnel costs, there is a strong demand for ASVs. While Lagrangian monitoring has been widely used in oceanography using drifters (Subbaraya et al., 2016) and in atmospheric studies using balloons (Businger et al., 1996), its upfront, maintenance, and operational costs remain prohibitively expensive for the monitoring of surface freshwater ecosystems. Currently, most commercially available ASVs for freshwater ecosystems are adaptations of ASVs used in oceanography, which has resulted in large-size and costly vehicles (e.g., the Teledyne Z-Boat 1800RP).

The advantages brought by Lagrangian monitoring can be better explained by comparing Eulerian and Lagrangian monitoring of a marathon race and the propagation of a disturbance in a river corridor. After the start of the events, Eulerian monitoring helps quantify what happens over time at fixed cross-sections, such as the finish line or a bridge. Therefore, Eulerian-based statistical analyses are limited to piece-wise rankings, histograms (or probability density functions), percentile analyses, and averages. On the other hand, Lagrangian monitoring would let us link spatiotemporal variations of relevant quantities such as stride length, cadence, heart rate, vertical oscillation, ground contact time, and speed for a runner, or temperature, dissolved oxygen, turbidity, and other water quality parameters changing as the disturbance moves downstream. The only requisite is that runners and rivers 'wear' sensors. From those individual quantities and the relationships among them, e.g., change of heart rate as a function of change in elevation and change in dissolved oxygen levels as a function of turbidity, more robust spatiotemporal analyses can be performed to characterize a runner's performance during a marathon or a river's response to a disturbance.

The practical limitations of Lagrangian monitoring include: 1) currently, we can instrument only one or a few parcels of water, and we end up effectively disregarding the rest of them; 2) until we can deploy smart aquatic nanobots, the size of our Lagrangian-based technologies will continue to define the flow paths they follow and the aquatic systems where they can be used; 3) Lagrangian-based monitoring cannot easily distinguish the effects of spatial and temporal variability on biogeochemical processes, particularly if the temporal extent of the monitoring overlaps with dominant diel or seasonal fluctuations (Ensign et al., 2017).

Since most of the progress made to date in the study and management of freshwater ecosystems is based on the use of Eulerian monitoring, any productive discussion about ways to improve the monitoring of freshwater ecosystems should consider strengthening the capabilities of existing infrastructure. For example, there are over 10,000 USGS streamflow stations around the US, and some are also instrumented with water quality sensors ("USGS WaterWatch – Streamflow conditions," n. d.). However, to our knowledge, there is no active program pursuing Lagrangian-based monitoring between sites located along river corridors. Integrating more traditional Eulerian monitoring sites with Lagrangian capabilities, thus, can help researchers, consultants, and stakeholders better understand *where, how*, and *why* water quality and quantity change in time and space (Ensign et al., 2017; Griffiths et al., 2022; Hensley et al., 2020).

In this article, we present the development of an ASV, *The Navigator*, with sensing technology to collect and transmit water quality data in real-time over spatial and temporal scales that are currently uncommon, i.e., at the sub-minute scale and following flow currents or GPS waypoints. We describe the components and architecture of The Navigator and demonstrate its applicability in the Lagrangian monitoring of surface water bodies in New Mexico (USA) to: 1) identify water quality changes associated with land use changes along a 7th-order reach in the Rio Grande, 2) identify the fate of wildfire disturbances ~175 km downstream of a burned watershed affected by the largest wildfire ever recorded in the state, 3) monitor the water quality of a recreational fishing pond in the City of Albuquerque.

2. Methods

2.1. The Navigator: overview

The Navigator features a GPS tracker to monitor spacetime variations and to allow the recovery of the vehicle, a thruster and rudder system that can be automated using an autopilot, a data logger that can be coupled to water quality sensors (i.e., optical, wet chemistry, fluorometers), and real-time data transmission capabilities through LTE cellular service. The Navigator is ideal for Lagrangian monitoring applications in river systems without major obstructions, irrigation and drainage channels, and lentic systems (e.g., lakes, reservoirs, estuaries). The Navigator can monitor water quality parameters over longer durations than other ASVs commercially available, is lighter than other alternatives (2.5–5x lighter), and can be coupled to different sensor heads, offering high versatility. Fig. 1 and Table 1 present all parts included in The Navigator and their assemblage to make the system work. Supplementary Information A1 provides access to a 3D-CAD view of The Navigator.

2.2. Structure and hardware design

We used a catamaran (i.e., twin hulls) framework to create a small-size vehicle with minimum flow resistance, better stability, and higher payload (Ferri et al., 2015). Each hull (C1 in Table 1) is made of expanded polystyrene (XPS) foam and has three layers of fiberglass outside. The two hulls are connected by a carbon fiber rod structure using 3D-printed brackets attached to the hulls (C2 in Table 1). A Pelican box (C3) houses electronics and batteries and is fastened to the front two carbon rods (C1). The thruster (C4) and servo (C5) with rudder are mounted on the back rods (C1). Since the vehicle's weight is distributed over two hulls, The Navigator has a shallow draft of 125 mm.

The thruster (C4) can provide a thrust force of ~3 kg, supporting a static positioning or navigation against the current when flow velocities are <0.8 m/s. The digital servo (C5) controls the steering, using a dual

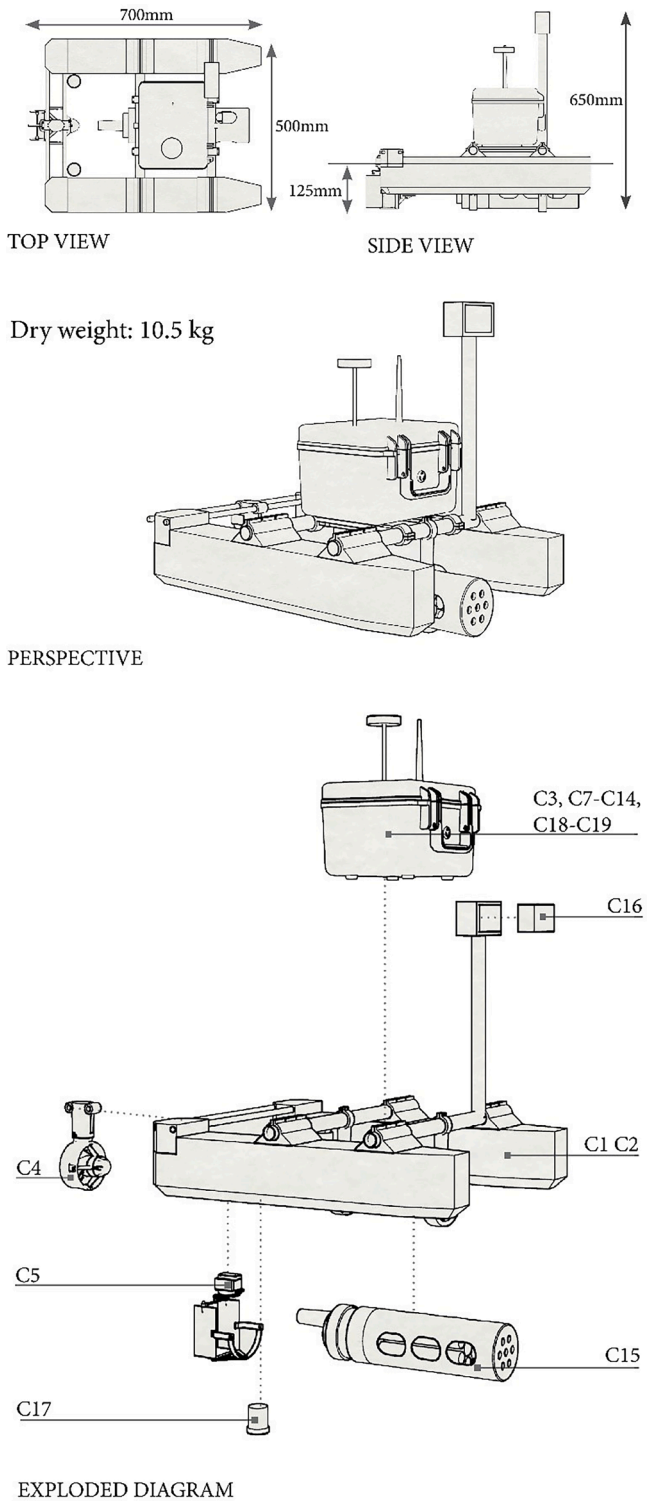

Fig. 1. The Navigator: parts, design and exploded diagram. Part descriptions are available in Table 1 and 3D view is available in Supplementary Information A1.

rudder design capable of providing sharp turns (0.75 m turning radius). The servo's maximum torque is up to 21.5 kg/cm @6.8 V. The dual rudder system (C2) connected to the servo was designed and manufactured by us and is 3D printable. The thruster is fixed, while the rudder is mounted directly behind the thruster.

The Navigator has two maneuvering modes: 1) drift mode, controlled by the operator, and 2) autonomous mode, following GPS waypoints. For drift mode, the operator controls a radio transmitter (C6). The commands sent by the operator are received by the radio control receiver (C7).

During autonomous mode, the autopilot (C8) gets continuous geolocation, roll, pitch, and heading data from GPS data (C9). This allows it to hold the course and follow GPS waypoints. The user can change between autonomous and drift modes using a switch on the controller (C6). The geolocation, depth, roll, and pitch information are transferred continuously to the user using a telemetry transmitter with a range of ~5 km (C10), which can be affected by terrain factors blocking or reflecting radio waves, and a matching receiver (C10) attached to a field laptop. Power is supplied to The Navigator through four packs of lithium polymer batteries (C11). In our tests, this power provided a range of ~30 km in autonomous mode. A small solar panel (C12) and a controller (C13) were added to extend the battery's capacity. Lithium batteries (C11) were selected because they provide a better weight-energy density ratio, high performance, and longevity. A 12 V power converter is used to supply the sonde, and a 5 V power converter is used to power the servo (C5) and the microcontroller board Raspberry Pi (C14).

The Navigator includes a multiparameter water quality sonde Yosemitech - Model Y4000 (C15). We chose this sonde due to its compact size, low cost, and ease of integration. The Y4000 monitors dissolved oxygen, conductivity, turbidity, pH, chlorophyll, and temperature. An integrated wiper system can prevent biofouling, air bubbles, and debris, thus reducing erroneous data. The multiparameter sonde is controlled using the Raspberry Pi board (C14) to define temporal resolution, deploy the sensor heads, and save data files. The sonde can be calibrated using the multi-sensor PC tool by Yosemite Technologies.

The Navigator features an OAK-D Lite 13MP depth camera (C16) to collect field photographs and a 30-degree single-beam echosounder ping sonar (C17) to measure depth. The camera is connected to the Raspberry Pi board (C14) and the sonar is connected to the autopilot (C8). The Navigator has an LTE modem with a cellular SIM card (C18) connected to the Raspberry Pi (C14) to transfer real-time data that can be shared worldwide. Finally, penetrators (C18) are used to have watertight seal electrical cables as they pass into the pelican case (C3).

2.3. Software design

The Navigator software provides easy-to-replicate and customized monitoring solutions to a broad range of users, and all our code is publicly hosted on GitHub (see Supplementary Information A2). The Navigator uses an Ubuntu Desktop 22.04.1 LTS Linux operating system running on the Raspberry Pi 4 4GB (C14). The software is designed as a set of Robot Operating System 2 (ROS2) nodes. To understand the architecture of our software, it is necessary to understand the ROS2 ecosystem it is built on. When using ROS2, the code is organized into packages containing nodes based on their function, and those nodes communicate with each other through messages. The nodes create and observe such messages by publishing and subscribing to specific topics. This provides flexibility, as users can integrate additional ROS2 packages to fit their needs without modifying already integrated nodes. Within the code developed for The Navigator, we have several nodes responsible for a task onboard the vehicle. Fig. 2 presents the architecture of our software, with representative titles for the roles of the nodes and connections showing the topics that the nodes communicate through publishing and subscription.

The Autopilot system uses ArduPilot's ArduRover version 3.5.2 firmware. The Autopilot requires setup and calibration tasks, which are well-documented on the ArduPilot website. The operator needs to install a ground station on their field laptop to communicate with the Cube autopilot (C8) through the telemetry radio (C10). The data transmitted include GPS waypoints, battery health, the autopilot's sensor health, etc. We used ArduPilot's Mission Planner software because it is the most popular and has an extensive database with community support and

Table 1
The Navigator component description and costs in USD, as of May 2023.

Part	Name	Image	Description	Cost (YY 2023 USD)
C1	Hull: Fiberglass with Foam and carbon fiber rods	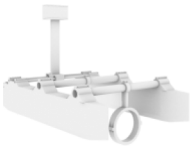	An insulation foam sheet with a thickness of 5.1 cm is used for the hull's shape. Three layers of fiberglass cloth (50 m^2) were coated outside using epoxy resin and hardener (250 ml). Carbon fiber rods are used as beams.	$110
C2	3D printed components		Approximately 1 kg of acrylonitrile butadiene styrene (ABS) filament was used for 3D printing the rudder and carbon rod connections to provide durability and UV resistance to The Navigator.	$22
C3	Protector case: Pelican		This rugged case features an automatic purge valve that equalizes air pressure, and a watertight silicone O-ring lid. This case protects all the hardware in The Navigator from impacts and water splashes.	$80
C4	Thruster: Blue Robotics T200		The T200 thruster is a popular underwater thruster used for The Navigator. Its flooded motor design makes it powerful, efficient, compact, and affordable.	$236
C5	Digital Servo: Annimos 20KG with 5 V power converter		This Annimos 20KG digital servo with high torque and full metal gear is waterproof and helps control the steering of The Navigator with a control angle of 270°	$16
C6	Radio Transmitter: Emax E8		A 2.4 GHz dual band antenna radio transmitter features an 8 channel RF module.	$59
C7	Radio Control Receiver: RadioMaster R88		2.4 GHz radio control receiver for remote control, with a range of ~1 km.	$20
C8	Autopilot: Cube purple with mini carrier		This autopilot is designed to control boats, cars, or rovers. It provides hardware and an embedded software ecosystem to automate autonomous maneuvering in The Navigator.	$340
C9	GPS: Here 3		This GPS is a high-precision global navigation satellite system (GNSS) that supports real time kinematic (RTK) positioning and is built with controller area network (CAN) protocol. It is also designed to be dust-proof and splash-proof, which is ideal for The Navigator.	$125
C10	Telemetry Radio Transmitter and Receiver: 3DR		915 MHz transmitter and receiver, responsible for relaying images between the ASV and ground station computer with a range of 3–5 km.	$88

(*continued on next page*)

Table 1 (*continued*)

Part	Name	Image	Description	Cost (YY 2023 USD)
C11	Lithium polymer battery: Ovonic		Set of 4 Lithium polymer batteries, Voltage: 11.1 V, Cell: 3S, Capacity: 5500mAh, Discharge: 50C. These batteries power every component of The Navigator.	$55
C12	Solar panel: Eco Worthy 25 W 12 V		Waterproof solar panel 41.9 cm x 32 cm capable of providing 25 W. This panel helps extend battery life.	$36
C13	Solar Charge Controller: GV-5		This controller acts as an interface between the solar panel and the batteries, preventing them from overcharging.	$99
C14	Micro controller: Raspberry Pi 4		The Raspberry Pi 4 is a powerful, user-programmable microprocessor board that can be easily programmed with several popular IDE software programs like Linux. It includes LTE and Bluetooth communications for The Navigator.	$100
C15	Multiparameter sonde: Yosemitech Y4000		The Yosemitech Y4000 multi-parameter sonde is one of the most comprehensive and affordable water quality monitoring products available to monitor dissolved oxygen, conductivity, turbidity, pH, chlorophyll, blue-green algae, and temperature.	$3100
C16	Spatial AI stereo camera: OAK-D Lite		The OAK—D Lite is a spatial AI powerhouse, capable of simultaneously running advanced neural networks while providing depth from two stereo cameras.	$149
C17	Ping Sonar: Blue Robotics		The Ping Sonar is a single-beam echosounder that measures distances of up to 50 m underwater. A 30° beam width and an open-source software interface make it a powerful tool for The Navigator.	$360
C18	LTE modem dongle: ZTE MF833V		4 G LTE USB modem dongle provides a mobile internet connection to the Raspberry Pi and real-time data transfer.	$50
C19	Penetrator: Blue Robotics WetLink		This item is used to seal electrical cables as they pass into a component or through a pelican case. Each set includes a bulkhead, seal, plug, O-ring, and nut.	$56
Total cost (YY 2023 USD)				**$5101**

documentation. Other options include APM Planner and QGroundControl, among others. No modification of The Navigator source code is required to switch between ground stations.

The ground station, which may be housed at an onshore building, a mobile unit, or a boat, is crucial for deploying The Navigator. The ground control station's primary equipment is a laptop with ground control software installed. Additional components are a USB telemetry transmitter (C10) connected to the computer and an RC transmitter (C6). Wireless communication methods via telemetry transmitters are generally used to assign missions to The Navigator. The ground station keeps track of the status of The Navigator and its onboard hardware and sends control instructions to remotely operated missions.

We used Ubidots to create a website to communicate with The Navigator and visualize and download data. Ubidots provides a free tier for educational use and is easy to set up. We created a simple interface for viewing previous data over a wide time range, visualizing real-time updates when data are received, and restricted viewing access as specified by the user. Any website using HTTP could be used to communicate with The Navigator, but some slight modification of The Navigator source code would be necessary. The data sent to the website includes sonde readings, camera status, and GPS locations. Data are displayed as time-series plots with colored ranges and a map with pinpoints. The data are sent through the onboard USB LTE modem (C18).

We used the Luxonis Depth AI platform to save images taken from the Oak D lite camera (C16) in The Navigator. This platform combines artificial intelligence, computer vision, depth perception (Stereo, ToF), and segmentation. We programmed Luxonis Depth AI to save images for our initial field tests.

2.4. Assembly and modifications

The Navigator uses mainly off-the-shelf parts (Table 1), and the open-source code controlling the hardware is available via GitHub (Supplementary Information A2). However, assembling The Navigator from scratch or modifying its functioning (as described here) requires technical familiarity with electronics, programming, and mechanics. There could be support provided through the ArduPilot and Arduino communities.

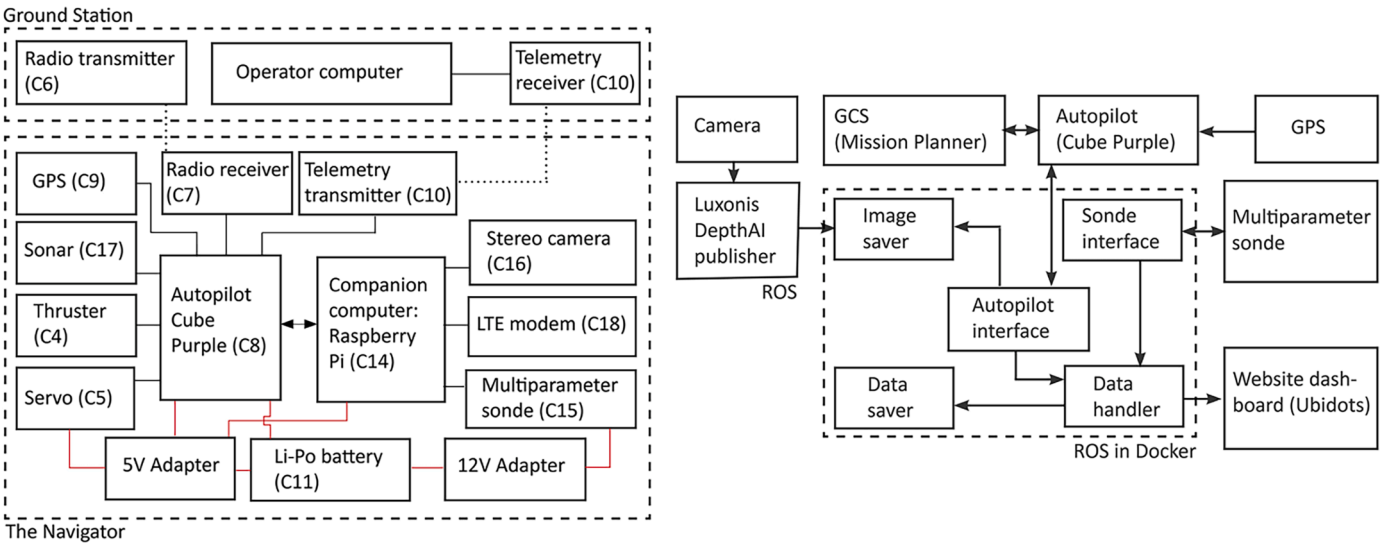

Fig. 2. The Navigator hardware (left) and software schematic (right).

Some customization options to modify the version of The Navigator presented here include choosing different types of sensors compatible with Arduino, changing the structural frame to suit specific water monitoring needs, and replacing the thruster and batteries to increase the power of the vehicle. Overall, the degree to which The Navigator is customizable depends on the sensors and components to be replaced and the technical expertise and resources available to the user.

3. Validation and field testing

We tested The Navigator in three applications. First, the Lagrangian monitoring of a 7th-order river reach in the Rio Grande using the drifting mode to understand where, how, and why water quality changes. Second, we monitored Santa Rosa Lake following GPS waypoints to characterize post-fire disturbances from the largest recorded wildfire in New Mexico, i.e., the Hermit's Peak-Calf Canyon wildfire that occurred in the spring of 2022. Third, we monitored a small urban detention pond in the City of Albuquerque using the autonomous mode to collect high spatial resolution water quality data and depth along a grid path.

Before each field day, we calibrated each sensor following the manufacturer's recommendations. With the field information collected from water quality sensors and GPS data, we generated heatmaps using R's spacetime and trajectories package (Pebesma, 2016). These heatmaps (KMZ graphic format) were later imported into Google Earth to create layered water quality maps to display water quality data in a Lagrangian framework.

3.1. The Navigator: drifting mode operation

On May 19 (day 1) and May 20, 2022 (day 2), we monitored 28.5 km of the Rio Grande near the City of Albuquerque in drifting mode, i.e., moving with the river's current. The watershed draining area is ~37,221 km^2 and features ~55% shrub and grassland, 36% forest, and ~2.8% developed land (Khandelwal et al., 2020; Regier et al., 2020). The study reach starts ~58 km downstream of Cochiti Lake, a flood and flow control reservoir that removes sediment from the river (Massong et al., 2010). This section of the river features the City of Rio Rancho's wastewater treatment plant (WWTP) return effluent, the City of Albuquerque's water intake for drinking supply, storm and agricultural return flow channels, and the City of Albuquerque's WWTP return effluent (Fluke et al., 2019). Due to low flow conditions, i.e., 21.8 m^3/s compared to a 30-year median of 70.0 m^3/s (USGS gage 08330000), we were not able to collect data along a 15.3 km reach between Montaño Bridge and Rio Bravo Bridge (Fig. 3A) because the flow was too shallow and unsuitable for The Navigator. The United States Geological Survey (USGS) operates several stream gages in this reach, i.e., USGS 08329918 at Alameda Bridge, USGS 08329928 near Paseo Del Norte Bridge, and USGS 08330830 at Valle de Oro, which we used to report flow data.

We collected data every 2-min for 5 h and 48 min on day 1 and for 4 h and 52 min on day 2. This corresponded to an average of one sampling event every 114 m on day 1 and every 80 m on day 2. The Navigator collected GPS, turbidity, pH, temperature, dissolved oxygen (DO), and specific conductivity (SC) data (Fig. 4 and Figure S1). We activated the remote steering controller only when the vehicle was drifting near thick riparian vegetation and near the diversion dam used by the water treatment plant's intake facility. We followed The Navigator using a kayak through the study reaches and verified the functioning of real-time data telemetry with the Ubidots website dashboard.

The data collected by The Navigator revealed spatial and temporal changes in water quality parameters that would not be identifiable through Eulerian monitoring (Fig. 4). On day 1, we observed an increase in water temperature from 17.0 to 22.6 °C, which may be due in part to daily changes in air temperature over the monitoring period. We also observed a longitudinal increase in specific conductivity from 273.3 to 291.7 µS/cm, with abrupt changes near releases from the WWTP of the City of Rio Rancho (i.e., 273.8 to 299.6 µS/cm) and runoff outlets from unlined channels or arroyos (i.e., 281.3 to 290.4 µS/cm). These changes were local, as lateral discharges were orders of magnitude smaller than that from the Rio Grande, e.g., ~0.3 m^3/s was the effluent discharge from the Rio Rancho WWTP while 23.4 m^3/s was the discharge in the river. During our monitoring, the inflatable diversion dam controlling the water intake from the Rio Grande into the water treatment plant of the City of Albuquerque was raised and created water stagnation upstream and high turbulence downstream. To avoid the dam, we directed The Navigator to the fish bypass channel and detected changes in turbidity from 33 to 37 FNU upstream to 40–49 FNU downstream.

On day 2, The Navigator registered drastic water quality changes as it passed through the Albuquerque WWTP outfall, which has a maximum capacity of 76 MGD (i.e., 3.3 m^3/s). That day, the Rio Grande's average flow was 18.9 m^3/s, and the ABQ WWTP effluent discharge was 2.3 m^3/s. We recorded specific conductivity values increasing from 276.1 to 689.8 µS/cm and temperatures rising from 18.7 to 22.9 °C (Fig. 4). The temperature and conductivity values gradually decreased downstream of the WWTP point source for ~ 4 km and then rose gradually as a part of a diel cycle. Similarly, The Navigator registered changes in DO from 6.5 to 5.3 mg/L, turbidity from 53.1 to 8.8

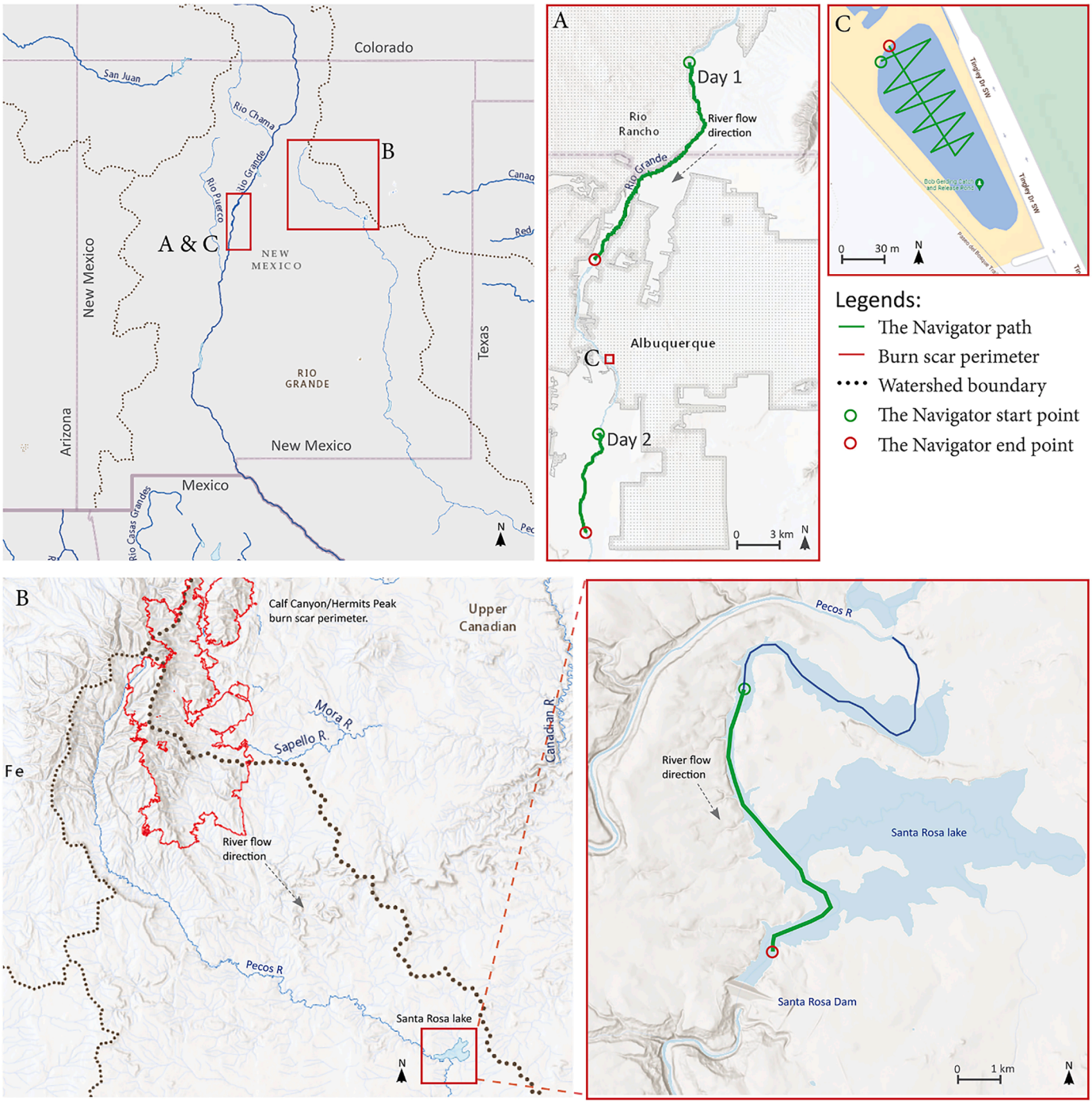

Fig. 3. A Map of New Mexico, USA, with red boxes enclosing the study sites. A) 7th-order study reach along the Rio Grande where The Navigator was used in drifting mode. B) Hermit's Peak-Calf Canyon Fire perimeter in red and boundaries of the impacted watershed draining to Santa Rosa Lake. The Navigator was deployed in autonomous mode to follow GPS waypoints across the lake. C) Recreational fishing pond in the City of Albuquerque, where The Navigator was deployed in autonomous mode following a grid pattern. (For interpretation of the references to colour in this figure legend, the reader is referred to the web version of this article.)

FNU, and pH from 8.1 to 7.1. These values also gradually rose to those upstream of the Albuquerque WWTP.

This study shows how The Navigator can monitor water quality parameters at higher spatial and temporal resolutions, supporting the identification of sources and the assessment of their impacts at spatial scales unattainable by Eulerian monitoring or synoptic grab sampling. In an ongoing study with The Navigator in this reach, we are quantifying how the variability of water quality parameters and fluxes from the river and the ABQ WWTP define longitudinal mixing lengths. For this, we are performing synchronous monitoring of the two river banks over contrasting river:WWTP flow ratios, and analyzing the data to identify where the differences in water quality parameters become negligible between the two banks, which are ~100 m apart. Since Eulerian monitoring requires a pre-defined selection of monitoring locations both longitudinally and transversally, the study of mixing lengths exemplifies one of multiple cases where Lagrangian monitoring with The Navigator would be more ideal and cost-effective than Eulerian monitoring.

Given the size of The Navigator, its use in flowing waters is much

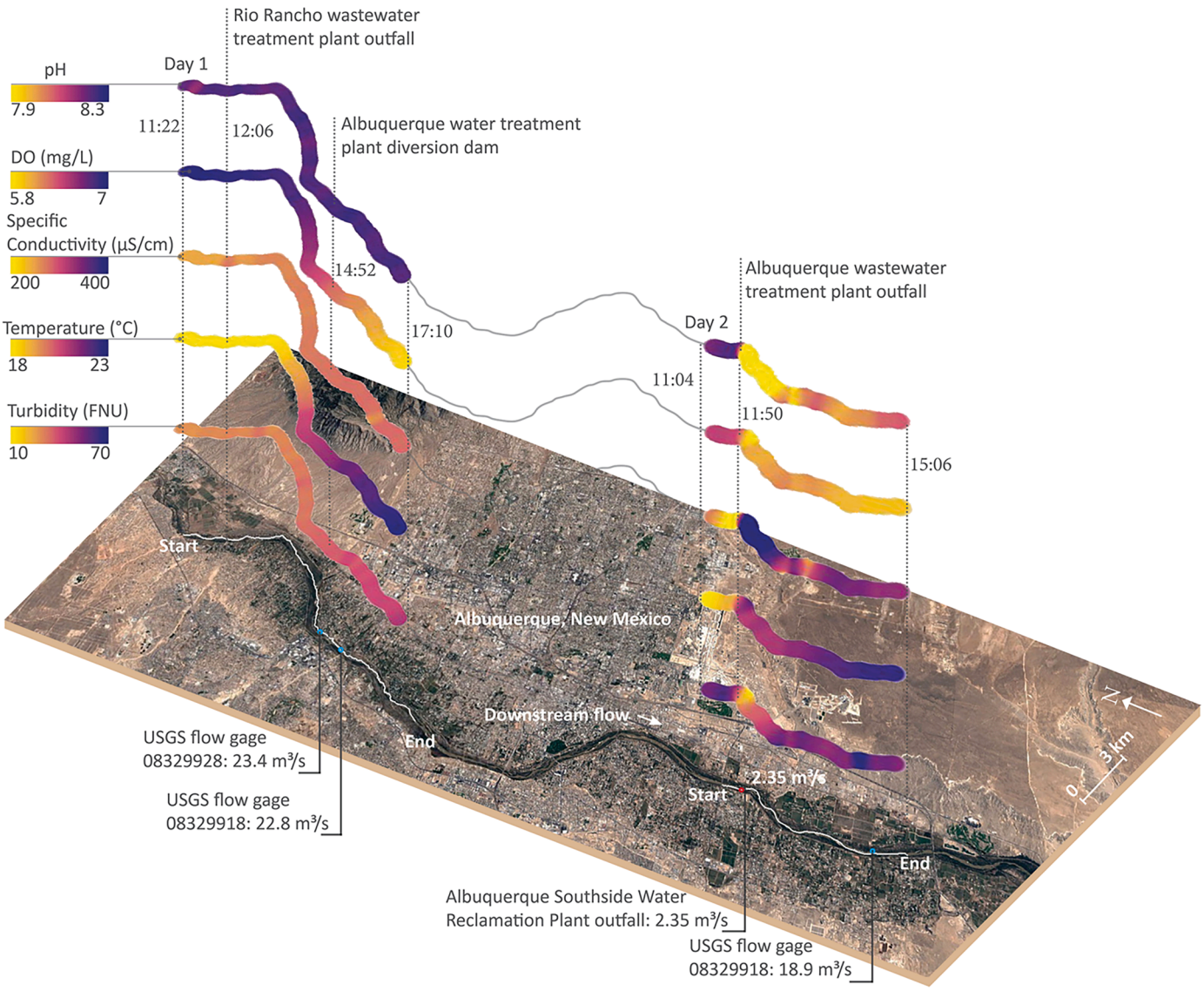

Fig. 4. Longitudinal heatmap profile of water quality parameters collected by The Navigator along a 7th order stream reach in the Rio Grande River near Albuquerque, NM. The blue dots indicate USGS flow gages and clock time is indicated in hh:mm. (For interpretation of the references to colour in this figure legend, the reader is referred to the web version of this article.)

more practical in less turbid and unobstructed segments of streams, rivers, and canals. From a mass or energy balance perspective, The Navigator is ideal for identifying patterns and processes not dominated by strong diel cycling, particularly if the navigation time overlaps with those timescales. Note, however, that The Navigator is nothing but a witness to the dynamic changes experienced by water parcels moving over space and time. Therefore, the Lagrangian data it collects represents what happens in the fluvial system and can be interpreted or modeled using appropriate boundary and initial conditions, some of which Eulerian monitoring can help better constrain. With this in mind, The Navigator is a technology that simplifies the identification of sources of physical (e.g., thermal) or biochemical pollution (e.g., unregulated sewage, non-compliant sewage, industrial or agricultural pollution), and can be integrated with other monitoring efforts to improve our understanding of how physical (e.g., water levels, temperature), chemical (e.g., water quality parameters), and biological indicators (e.g., vegetation, invertebrate, and fish abundance) of ecosystem health correlate over spatiotemporal scales.

3.2. *The Navigator: autonomous mode operation*

3.2.1. *Following GPS waypoints*

The Navigator is equipped with an autopilot system capable of following GPS waypoints to track water quality changes autonomously. With support for site access from the US Army Corps of Engineers (USACE) Albuquerque District, we conducted a high-resolution Lagrangian monitoring of water quality changes associated with the mobilization of wildfire disturbances after the Hermit's Peak-Calf Canyon Fire (Fig. S2). To contextualize, as of early 2023, this wildfire is the largest ever recorded in New Mexico and burned 138,188 hectares between April and June 2022. The fires began from out-of-control prescribed burns ("Hermit Peaks Fire," 2022) and expanded aggressively due to sustained high-wind and dry conditions that are part of a climate change-induced megadrought gripping vast areas of the western United States (Ball et al., 2021; Freedman and Fears, 2020). Postfire, after the storms from the monsoon season started to mobilize burned materials from the burned area into Gallinas Creek and into the Pecos River, we monitored water quality from Santa Rosa Lake and its upstream delta, which are located ~175 km downstream from the burn scar perimeter.

Since our goal was to determine how the discontinuity of a river system brought by a flow-regulating dam impacts the propagation of wildfire disturbances in a fluvial network, we monitored the Pecos River Delta-Santa Rosa Lake transition for ~8 km at a fine sampling spatial scale of about one sample every 64 m. The study was conducted on August 19, 2022, after a precipitation event of 9.4 mm fell over the burn scar on August 17–18, 2022 (USGS Atmosphere gage 354150105275301) and mobilized debris and sediments. The longitudinal monitoring followed the direction of the flow, which was 13.1 m^3/s, exceeding the median of 1.0 m^3/s between 1977 and 2022 (USGS gage 08382650) ("USGS WaterWatch – Streamflow conditions," n.d.).

The Navigator's data revealed drastic changes in the spatial patterns of water quality parameters (Fig. 5). DO transitioned from ~ 6 mg/L in the Pecos River upstream of the delta, into anoxic conditions (~0 mg/L) near the delta, and then rose as the water reached the dam. The DO sag and recovery patterns are inversely proportional to the turbidity values, suggesting that microbial respiration or chemical oxygen demands (DO sink) and photosynthesis (DO source) were largely controlled by sediment fluxes from the wildfire (Ball et al., 2021; Smith et al., 2011; Reale et al., 2015). pH values were lower in zones with low DO, suggesting increased aerobic microbial metabolism and CO_2 releases associated with the high influx of sediment from wildfire material (Chapra, 2008). Specific conductivity and temperature increased along the flow path following the DO trend. During the monitoring activity, we saw high sediment loads coming from Gallinas Creek and the Pecos River sinking along the delta due to the reduced flow velocity and the corresponding sedimentation (Drummond et al., 2018). We also saw floating debris and bubbles from wildfire disturbances remaining near the surface of the lake.

Our monitoring with The Navigator indicated drastic changes in water quality parameters over short distances along the lake in response to post-wildfire rainfall-runoff events occurring hundreds of kilometers upstream. This allowed us to identify hotspots and plausible sources and sinks of physicochemical parameters. Since the monitoring lasted <2 h, our data from the lake are not as affected by diel cycles as those from the Rio Grande. This study with The Navigator helped us understand how lakes affect the longitudinal propagation of wildfire disturbances along fluvial networks, acting as sinks and resetting the mobilization of wildfire material that there becomes part of the lakebed. Our results bring into focus the importance of Lagrangian monitoring and highlight the importance of selecting adequate sampling locations and spatial coverages.

Given the transient nature of the propagation of wildfire disturbances into Santa Rosa Lake, The Navigator proved to be an optimal tool for performing on-demand research through rapid response efforts. Even though Eulerian monitoring sites located upstream and downstream of the lake could have informed net changes occurring, The Navigator provided the geolocated data needed to understand complex physical and biochemical processes without relying on black-box approaches. In summary, The Navigator helped us know what happened along the lake, similar to what we could have learned using Eulerian monitoring, but also provided extra bits of essential information needed to understand where, why, and how the transition between the Pecos River and Santa Rosa Lake prompted such drastic changes in physicochemical characteristics that were relevant locally and along an entire fluvial network.

3.2.2. Following a grid path

On November 11, 2022, we deployed The Navigator in a recreational fishing pond in the City of Albuquerque (Figure S3). We used a GPS grid path mission of 400 m to monitor the north side of the pond using Mission Planner. This monitoring activity lasted 25 min, was completed at an average speed of 0.27 m/s, and used a sampling frequency of one sample per minute, amounting to about one sample every 16 m. The Navigator monitored turbidity, pH, temperature, DO, conductivity, oxygen reduction potential (ORP), and chlorophyll-A. We also added the depth sonar and an Oak D-lite camera. We chose a zig-zag grid path to gather high spatial resolution of water quality parameters and test the vehicle's maneuverability.

As expected, we observed minimum changes in surface water quality parameters due to the small size of the pond and the short duration of our test (Fig. 6). Even though the pond is relatively deep with respect to its surface area, the sensors in The Navigator cannot reach deeper layers to detect vertical heterogeneities. The values observed in this short study fall within expectations for low sediment, small ponds. Logistically, this test is analogous to monitoring a point source or the confluence of two streams. Thus, the autonomy of The Navigator would allow researchers and practitioners to monitor wide water bodies from a single location while collecting high spatial resolution data on water quality parameters and depth.

After exemplifying possible uses of The Navigator to monitor aquatic systems, we highlight here that its current version cannot monitor systems with depths smaller than 0.15 m and would struggle to navigate through narrow reaches with prominent boulders and vegetation extending over or under the surface water. Also, maintaining on-demand flow paths against stream and river currents greater than 0.8 m/s would require the addition of a more powerful thruster to increase its propulsion capacity, which would require bigger batteries, resulting in an overall bigger vehicle. Of course, that approach would deviate from our idea of creating a small autonomous vehicle that a small or one-person crew can handle. Therefore, we recommend using the autonomous mode in lakes or estuaries and the drift mode in streams and rivers.

3.3. The Navigator: comparison with existing technology

While numerous ASVs have been developed, most have focused on oceanography and only a few on freshwater applications. We compared the performance of The Navigator with three other monitoring platforms that were designed for longitudinal monitoring of freshwater systems: 1) the Xylem HYCAT, 2) the Teledyne Z-Boat 1800RP, and 3) the Oak Ridge National Laboratory (ORNL) AquaBOT (Griffiths et al., 2022). The spider map in Fig. 7 represents a qualitative comparison because a quantitative comparison would disregard the fact that they were built for different applications and can be custom-made. For example, the AquaBOT is designed specifically for the water quality monitoring of low-mid order streams and is ~2.5x times larger than The Navigator. The Teledyne Z-Boat 1800 is designed for hydrographic surveys that require higher payloads and is ~ 4–7x heavier (38–78 kg) and ~5x larger than The Navigator. The Xylems HYCAT can monitor bathymetry and water quality and is ~5x (53 kg) heavier than The Navigator.

4. Conclusions

The Navigator is an innovative, cost-effective (USD 5,101 in 2023), adaptable solution for Lagrangian monitoring of surface waters that can support progress in hydrologic sciences, watershed management, health, and wellbeing efforts worldwide. The Navigator can generate and share high spatial- and temporal-resolution water quality parameters, site photos, and depth surveys using off-shelf technologies that are affordable, open source, and easy to integrate with other sensor platforms. The off-the-shelf emerging technologies used are cutting-edge, making The Navigator smarter, cheaper, smaller, lighter, and more reliable than other ASV systems. The Navigator can generate and share data in real-time to help make informed decisions leading to improved environmental and human health outcomes, supporting the development of more sustainable and resilient societies.

Our field test data prove that The Navigator can help researchers, consultants, and stakeholders better understand the coupling of aquatic and human systems. It provides information to assist in planning, restoration, mitigation, enforcement, and disaster response efforts. The emphasis of this technology on understanding local-to-watershed scale spatial variations of natural and anthropogenic stressors can better inform holistic approaches for freshwater resource management. The

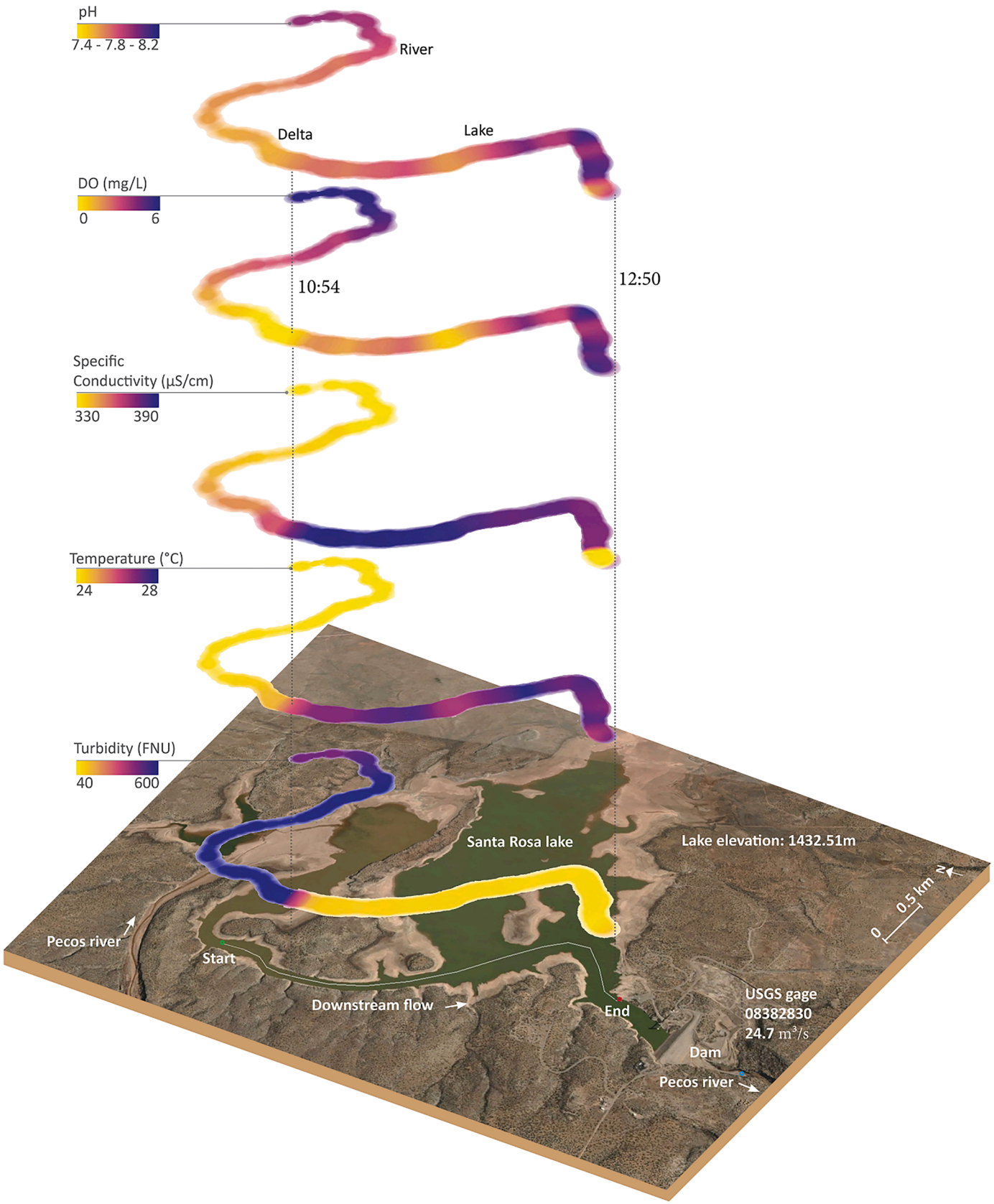

Fig. 5. The Navigator was used in autonomous mode to monitor water quality impacts from wildfire disturbances generated by the Hermit's Peaks-Calf Canyon fire in 2022. Santa Rosa Lake is located ~175 km downstream of the burn scar that is mainly drained by Gallinas Creek and the Pecos River. Clock time is in hh:mm.

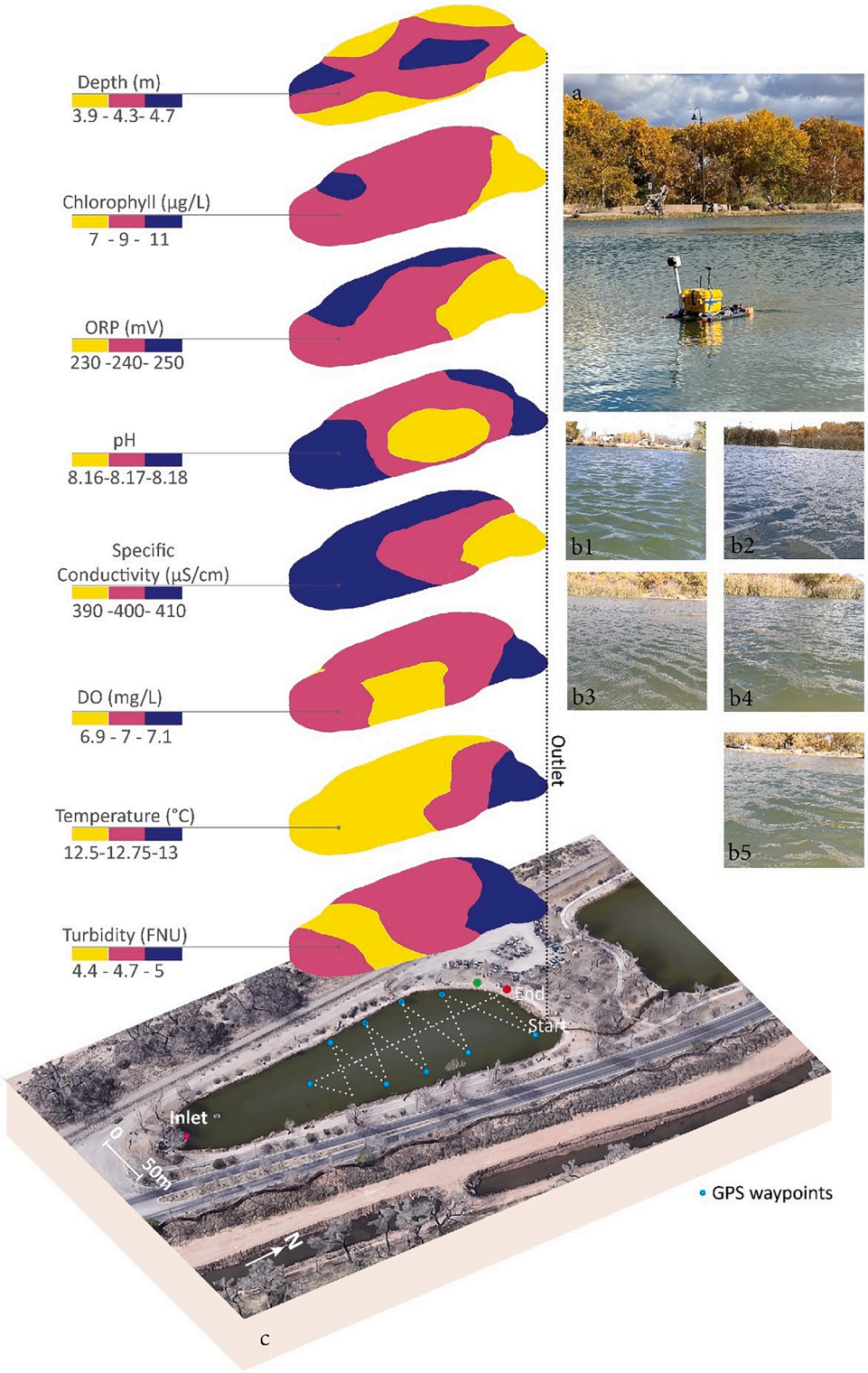

Fig. 6. a) The Navigator monitoring the Bob Gerding catch and release pond, Albuquerque, NM. b1-b5) Images captured by The Navigator while monitoring. c) Heatmap of the water quality parameters and depth data collected by The Navigator.

Navigator allows for sampling spatial heterogeneities in water quality parameters at sub-hour to multi-day resolutions, providing data-rich solutions with minimum upfront (Table 1), maintenance, and operational costs.

The Navigator facilitates the linkage between Eulerian datasets collected at a site (e.g., USGS stream flows and water quality data) and Lagrangian-based monitoring to provide a better understanding of where, how, and why spatiotemporal variation in water chemistry and biogeochemical processing occurs. This technology has numerous critical applications, primarily in the water, energy, and food sectors (i.e., across the food-energy-water FEW nexus in surface waters), as it provides high spatiotemporal resolution capturing the impacts of land use changes, point and diffuse sources, and the effects of climate variability on freshwater systems. The Navigator can help identify risks relevant to

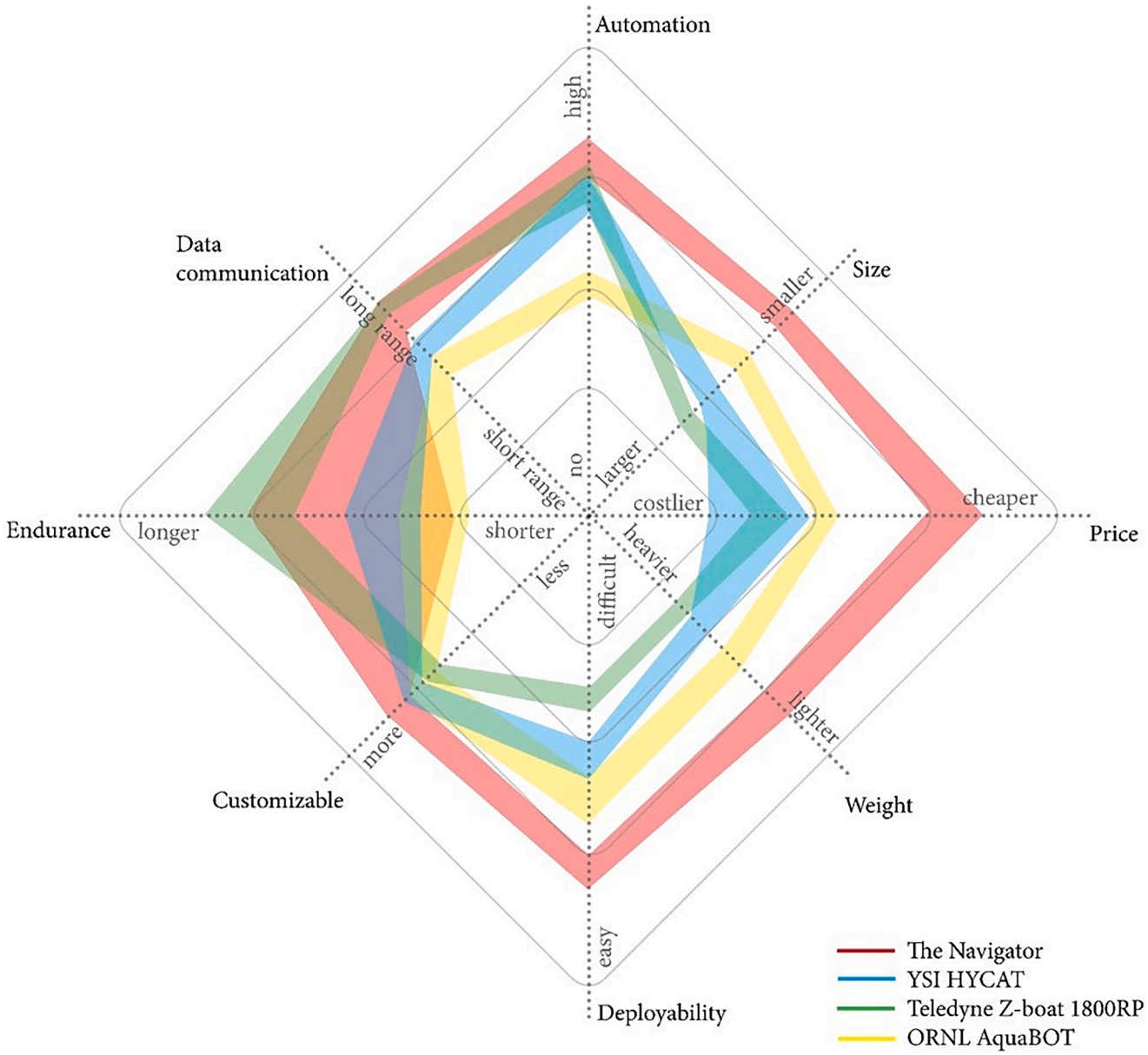

Fig. 7. Comparison spider map of three autonomous surface vehicle platforms and The Navigator.

the water supply for drinking, industrial, and agricultural activities and address concerns from the associated return flows (e.g., combined sewer overflows, thermal pollution, excess nutrients, etc.). This system can inform agencies about water quality issues related to excess loads, dilution requirements, unwanted leakages to aquatic ecosystems, and gaining and losing conditions in rivers and lakes. The spatiotemporal water quality data generated by this development can support the development of regulation and enforcement of environmental flows, thermal pollution, and mitigation and restoration efforts post-disturbance (e.g., wildfires, spills, land use changes, etc.). Overall, The Navigator can help address questions involving mass and energy balances in surface water ecosystems and support evidence-based decision-making.

Declaration of Competing Interest

Ricardo González-Pinzón reports financial support was provided by National Science Foundation and the New Mexico Water Resources Research Institute.

Data availability

Code is shared in Supplementary Information.

Acknowledgments

The National Science Foundation supported this research through grants CBET- 2054444 and HRD- 1914490. The New Mexico Water Resources Research Institute also supported this research. We thank David Van Horn (University of New Mexico), Justin Reale and Paul Sanchez (US Army Corps of Engineers) for their help coordinating access and field tasks in Santa Rosa Lake.

Supplementary materials

Supplementary material associated with this article can be found, in the online version, at doi:10.1016/j.watres.2023.120577.

References

Abbott, B.W., Gruau, G., Zarnetske, J.P., Moatar, F., Barbe, L., Thomas, Z., Fovet, O., Kolbe, T., Gu, S., Pierson-Wickmann, A.-C., Davy, P., Pinay, G., 2018. Unexpected spatial stability of water chemistry in headwater stream networks. Ecol. Lett. 21, 296–308. https://doi.org/10.1111/ele.12897.

Arabi, B., Salama, Mhd.S., Pitarch, J., Verhoef, W., 2020. Integration of in-situ and multi-sensor satellite observations for long-term water quality monitoring in coastal areas. Remote Sens. Environ. 239, 111632 https://doi.org/10.1016/j.rse.2020.111632.

Arsenault, R., Martel, J.-L., Brunet, F., Brissette, F., Mai, J., 2023. Continuous streamflow prediction in ungauged basins: long short-term memory neural networks clearly outperform traditional hydrological models. Hydrol. Earth Syst. Sci. 27, 139–157. https://doi.org/10.5194/hess-27-139-2023.

Ball, G., Regier, P., González-Pinzón, R., Reale, J.K., Van Horn, D.J., 2021. Wildfires increasingly impact western US fluvial networks: code and data archive. Zenodo.

Burns, D.A., Pellerin, B.A., Miller, M.P., Capel, P.D., Tesoriero, A.J., Duncan, J.M., 2019. Monitoring the riverine pulse: applying high-frequency nitrate data to advance integrative understanding of biogeochemical and hydrological processes. WIREs Water 6, e1348. https://doi.org/10.1002/wat2.1348.

Businger, S., Chiswell, S.R., Ulmer, W.C., Johnson, R., 1996. Balloons as a Lagrangian measurement platform for atmospheric research. J. Geophys. Res. Atmospheres 101, 4363–4376. https://doi.org/10.1029/95JD00559.

Chapra, S.C., 2008. Surface Water-Quality Modeling. Waveland Pr Inc, Long Grove, Ill.

Devaraj, S., Jenifa Latha, C., Geetha Priya, M., Jesudhas, C.J., Yarrakula, K., Panneerselvam, B., Pande, C.B., Muniraj, K., Balasubramanian, A., 2022. Hydrological modelling for ungauged basins: an overview of the past, present, and future directions. In: Ravichandran, N. (Ed.), Climate Change Impact On Groundwater Resources: Human Health Risk Assessment in Arid and Semi-Arid Regions. Springer International Publishing, Cham, pp. 313–327. https://doi.org/10.1007/978-3-031-04707-7_17.

Doyle, M.W., Ensign, S.H., 2009. Alternative reference frames in river system science. Bioscience 59, 499–510. https://doi.org/10.1525/bio.2009.59.6.8.

Drummond, J.D., Larsen, L.G., González-Pinzón, R., Packman, A.I., Harvey, J.W., 2018. Less fine particle retention in a restored versus unrestored urban stream: balance between hyporheic exchange, resuspension, and immobilization. J. Geophys. Res. Biogeosci. 123, 1425–1439. https://doi.org/10.1029/2017JG004212.

Dupas, R., Minaudo, C., Gruau, G., Ruiz, L., Gascuel-Odoux, C., 2018. Multidecadal trajectory of riverine nitrogen and phosphorus dynamics in rural catchments. Water Resour. Res. 54, 5327–5340. https://doi.org/10.1029/2018WR022905.

Ensign, S.H., Doyle, M.W., Gardner, J.R., 2017. New strategies for measuring rates of environmental processes in rivers, lakes, and estuaries. Freshw. Sci. 36, 453–465. https://doi.org/10.1086/692998.

Ferri, G., Manzi, A., Fornai, F., Ciuchi, F., Laschi, C., 2015. The HydroNet ASV, a small-sized autonomous catamaran for real-time monitoring of water quality: from design to missions at sea. IEEE J. Ocean. Eng. 40, 710–726. https://doi.org/10.1109/JOE.2014.2359361.

Fluke, J., González-Pinzón, R., Thomson, B., 2019. Riverbed sediments control the spatiotemporal variability of E. coli in a highly managed. Arid River. Front. Water 1.

Freedman, A., Fears, D., 2020. The western U.S. is locked in the grips of the first human-caused megadrought, study finds. Wash. Post.

Gabrielle, V., 2019. The Renaissance of Hydrology - Eos [WWW Document]. URL https://eos.org/features/the-renaissance-of-hydrology (accessed 9.26.19).

González-Pinzón, R., Dorley, J., Regier, P., Fluke, J., Bicknell, K., Nichols, J., Khandelwal, A., Wolf, E., Caruana, S.N., Horn, D.J.V., 2019. Introducing "The Integrator": a novel technique to monitor environmental flow systems. Limnol. Oceanogr. Methods 17, 415–427. https://doi.org/10.1002/lom3.10322.

Griffiths, N.A., Levi, P.S., Riggs, J.S., DeRolph, C.R., Fortner, A.M., Richards, J.K., 2022. Sensor-equipped unmanned surface vehicle for high-resolution mapping of water quality in low- to mid-order streams. ACS EST Water 2, 425–435. https://doi.org/10.1021/acsestwater.1c00342.

Hensley, R.T., Cohen, M.J., Korhnak, L.V., 2014. Inferring nitrogen removal in large rivers from high-resolution longitudinal profiling. Limnol. Oceanogr. 59, 1152–1170. https://doi.org/10.4319/lo.2014.59.4.1152.

Hensley, R.T., Spangler, M.J., DeVito, L.F., Decker, P.H., Cohen, M.J., Gooseff, M.N., 2020. Evaluating spatiotemporal variation in water chemistry of the upper Colorado River using longitudinal profiling. Hydrol. Process. 34, 1782–1793. https://doi.org/10.1002/hyp.13690.

Hermit Peaks Fire [WWW Document], 2022. URL https://inciweb.nwcg.gov/incident-information/nmsnf-hermits-peak-fire (accessed 2.5.23).

Huang, J., Borchardt, D., Rode, M., 2022. How do inorganic nitrogen processing pathways change quantitatively at daily, seasonal, and multiannual scales in a large agricultural stream? Hydrol. Earth Syst. Sci. 26, 5817–5833. https://doi.org/10.5194/hess-26-5817-2022.

Jarvie, H.P., Sharpley, A.N., Kresse, T., Hays, P.D., Williams, R.J., King, S.M., Berry, L.G., 2018. Coupling high-frequency stream metabolism and nutrient monitoring to explore biogeochemical controls on downstream nitrate delivery. Environ. Sci. Technol. 52, 13708–13717. https://doi.org/10.1021/acs.est.8b03074.

Khandelwal, A., González-Pinzón, R., Regier, P., Nichols, J., Van Horn, D.J., 2020. Introducing the SELF-CLEANING FILTRATION for WATER QUALITY SENSORS (SC-FLAWLeSS) system. Limnol. Oceanogr. Methods 18, 467–476. https://doi.org/10.1002/lom3.10377.

Kirchner, J.W., Neal, C., 2013. Universal fractal scaling in stream chemistry and its implications for solute transport and water quality trend detection. Proc. Natl. Acad. Sci 110, 12213–12218. https://doi.org/10.1073/pnas.1304328110.

Krause, S., Jörg Lewandowski, Clifford N. Dahm, Klement Tockner, 2015. Frontiers in real-time ecohydrology – a paradigm shift in understanding complex environmental systems - Krause - 2015 - Ecohydrology - Wiley Online Library [WWW Document]. URL https://onlinelibrary.wiley.com/doi/full/10.1002/eco.1646 (accessed 9.26.19).

Kunz, J.V., Hensley, R., Brase, L., Borchardt, D., Rode, M., 2017. High frequency measurements of reach scale nitrogen uptake in a fourth order river with contrasting hydromorphology and variable water chemistry (Weiße Elster, Germany): N in rivers-high frequency measurements. Water Resour. Res. 53, 328–343. https://doi.org/10.1002/2016WR019355.

Li, B., Yang, G., Wan, R., 2020. Multidecadal water quality deterioration in the largest freshwater lake in China (Poyang Lake): implications on eutrophication management. Environ. Pollut. 260, 114033 https://doi.org/10.1016/j.envpol.2020.114033.

Li, Wei, Xie, X., Li, Wanqiu, van der Meijde, M., Yan, H., Huang, Y., Li, X., Wang, Q., 2022. Monitoring of hydrological resources in surface water change by satellite altimetry. Remote Sens 14, 4904. https://doi.org/10.3390/rs14194904.

Lloyd, C.E.M., Freer, J.E., Johnes, P.J., Collins, A.L., 2016. Using hysteresis analysis of high-resolution water quality monitoring data, including uncertainty, to infer controls on nutrient and sediment transfer in catchments. Sci. Total Environ. 543, 388–404. https://doi.org/10.1016/j.scitotenv.2015.11.028.

Manfreda, S., McCabe, M.F., Miller, P.E., Lucas, R., Pajuelo Madrigal, V., Mallinis, G., Ben Dor, E., Helman, D., Estes, L., Ciraolo, G., Müllerová, J., Tauro, F., De Lima, M.I., De Lima, J.L.M.P., Maltese, A., Frances, F., Caylor, K., Kohv, M., Perks, M., Ruiz-Pérez, G., Su, Z., Vico, G., Toth, B., 2018. On the use of unmanned aerial systems for environmental monitoring. Remote Sens 10, 641. https://doi.org/10.3390/rs10040641.

Massong, T., Makar, P., Bauer, T., 2010. Recent channel incision and floodplain evolution within the middle rio grande, NM.

Matson, P.G., Stevenson, L.M., Griffiths, N.A., DeRolph, C.R., Jett, R.T., Fortner, A.M., Jones, M.W., Jones, N.J., Mathews, T.J., 2021. Multidecadal biological monitoring and abatement program\ assessing human impacts on aquatic ecosystems within the Oak Ridge Reservation in eastern Tennessee, USA. Hydrol. Process. 35, e14340. https://doi.org/10.1002/hyp.14340.

Nichols, J., Khandelwal, A.S., Regier, P., Summers, B., Van Horn, D.J., González-Pinzón, R., 2022. The understudied winter: evidence of how precipitation differences affect stream metabolism in a headwater. Front. Water 4.

Pebesma, E., 2016. Handling and Analyzing Spatial, Spatiotemporal and Movement Data [WWW Document]. URL https://edzer.github.io/UseR2016/#spatiotemporal-data-movement-data (accessed 1.18.23).

Reale, J.K., Van Horn, D.J., Condon, K.E., Dahm, C.N., 2015. The effects of catastrophic wildfire on water quality along a river continuum. Freshw. Sci. 34, 1426–1442. https://doi.org/10.1086/684001.

Regier, P.J., González-Pinzón, R., Van Horn, D.J., Reale, J.K., Nichols, J., Khandewal, A., 2020. Water quality impacts of urban and non-urban arid-land runoff on the Rio Grande. Sci. Total Environ. 729, 138443 https://doi.org/10.1016/j.scitotenv.2020.138443.

Rode, M., Wade, A.J., Cohen, M.J., Hensley, R.T., Bowes, M.J., Kirchner, J.W., Arhonditsis, G.B., Jordan, P., Kronvang, B., Halliday, S.J., Skeffington, R.A., Rozemeijer, J.C., Aubert, A.H., Rinke, K., Jomaa, S., 2016. Sensors in the stream: the high-frequency wave of the present. Environ. Sci. Technol. 50, 10297–10307. https://doi.org/10.1021/acs.est.6b02155.

Román, M.O., Stokes, E.C., Shrestha, R., Wang, Z., Schultz, L., Carlo, E.A.S., Sun, Q., Bell, J., Molthan, A., Kalb, V., Ji, C., Seto, K.C., McClain, S.N., Enenkel, M., 2019. Satellite-based assessment of electricity restoration efforts in Puerto Rico after Hurricane Maria. PLoS ONE 14, e0218883. https://doi.org/10.1371/journal.pone.0218883.

Smith, H.G., Sheridan, G.J., Lane, P.N.J., Nyman, P., Haydon, S., 2011. Wildfire effects on water quality in forest catchments: a review with implications for water supply. J. Hydrol. 396, 170–192. https://doi.org/10.1016/j.jhydrol.2010.10.043.

Subbaraya, S., Breitenmoser, A., Molchanov, A., Muller, J., Oberg, C., Caron, D.A., Sukhatme, G.S., 2016. Circling the seas: design of lagrangian drifters for ocean monitoring. IEEE Robot. Automat. Mag. 23, 42–53. https://doi.org/10.1109/MRA.2016.2535154.

Tapley, B.D., Watkins, M.M., Flechtner, F., Reigber, C., Bettadpur, S., Rodell, M., Sasgen, I., Famiglietti, J.S., Landerer, F.W., Chambers, D.P., Reager, J.T., Gardner, A.S., Save, H., Ivins, E.R., Swenson, S.C., Boening, C., Dahle, C., Wiese, D.N., Dobslaw, H., Tamisiea, M.E., Velicogna, I., 2019. Contributions of GRACE to understanding climate change. Nat. Clim. Change 9, 358–369. https://doi.org/10.1038/s41558-019-0456-2.

United Nations Environment Programme, 2021. Progress On Ambient Water Quality –2021 Update.

USGS WaterWatch – Streamflow conditions [WWW Document], n.d. URL https://waterwatch.usgs.gov/new/index.php (accessed 1.9.23).

Wieland, M., Martinis, S., 2019. A modular processing chain for automated flood monitoring from multi-spectral satellite data. Remote Sens. 11, 2330. https://doi.org/10.3390/rs11192330.